Energetics of Folding and DNA Binding of the MATα2 Homeodomain†

John H. Carra and Peter L. Privalov*

Department of Biology and Biocalorimetric Center, The Johns Hopkins University, Baltimore, Maryland 21218

Received August 28, 1996; Revised Manuscript Received November 5, 1996⊗

ABSTRACT: Homeodomains are a class of DNA-binding protein domains which play an important role in genetic regulation in eukaryotes. We have characterized the thermodynamics of folding and sequence-specific association with DNA of the MATα2 homeodomain of yeast. Using differential scanning and isothermal titration calorimetry, we measured the enthalpy, heat capacity, and Gibbs free energy changes of these processes. The protein−DNA interaction is enthalpically driven at physiological temperatures. DSC data on the process of melting the protein−DNA complex at different salt concentrations were dissected into its endothermic components, yielding the enthalpy change and dissociation constant of binding. A comparison of the circular dichroism spectra of the free and DNA-bound protein species revealed the formation of additional α-helical structure upon binding to DNA. We propose that the latter half of helix 3, the recognition helix, is substantially unfolded in the free protein under the conditions used, as has been observed with other homeodomains [Tsao, D. H. H., et al. (1994) *Biochemistry 33,* 15053−15060; Cox, M., et al. (1995) *J. Biomol. NMR 5,* 23−32]. Formation of protein structure is induced by DNA binding, and the energies measured for association therefore include a component due to folding.

The homeodomain is a small structural motif found in many proteins which regulate transcription in eukaryotes (Gehring et al., 1994). Many of these proteins have important roles in control of development, and in at least one case, homeodomain-containing DNA-binding proteins are involved in oncogenesis in humans (Kamps et al., 1990). Structures of several homeodomains have been solved (Qian et al., 1989, 1994; Kissinger et al., 1990; Wolberger et al.,-1991; Clarke et al., 1994; Cox et al., 1995; Hirsch & Aggarwal, 1995; Li et al., 1995; Tsao et al., 1995; Wilson et al., 1995) and have revealed a similarity to the prototypical helix−turn−helix motif of bacteria. The MATα2 protein of *Saccharomyces cerevisiae* contains a sequence-specific DNA-binding homeodomain joined to a dimerization domain by a flexible linker (Sauer et al., 1988; Wolberger et al., 1996). In conjunction with other proteins, including the MADS-box protein MCM1 (Smith & Johnson, 1992) and the homeodomain-containing MATa1 protein (Goutte & Johnson, 1993; Baxter et al., 1994; Phillips et al., 1994; Stark & Johnson, 1994; Li et al., 1996), the α2 protein functions to regulate expression of mating-type-specific genes.

The structure of the α2 homeodomain bound to DNA is shown in Figure 1 (Wolberger et al., 1991). It contains three α-helices, one of which (helix 3) lies in the DNA major groove and makes specific interactions with the bases and phosphate backbone. An N-terminal arm wraps around the back of the DNA to make contacts in the minor groove. In Figure 1, this arm as well as the C-terminal half of the recognition helix 3 are shown in gray, to indicate the induction of structure upon DNA binding. Evidence for an increase of structural order in the N-terminal arm has come from NMR spectroscopy (Phillips et al., 1991) and X-ray crystallography data (Wolberger et al., 1991), while we will present herein an argument that helix 3 is extended upon DNA binding. A 22-amino acid C-terminal extension of the protein is disordered in both the free protein and the crystal structure of α2 bound to DNA and is not shown. This portion of the molecule forms an additional α-helix when interacting with the MATa1 protein, as a1 is bound together with α2 on DNA (Baxter et al., 1994; Phillips et al., 1994). The α2 homeodomain produces only slight deviations from B-form in the DNA of the crystallized complex.

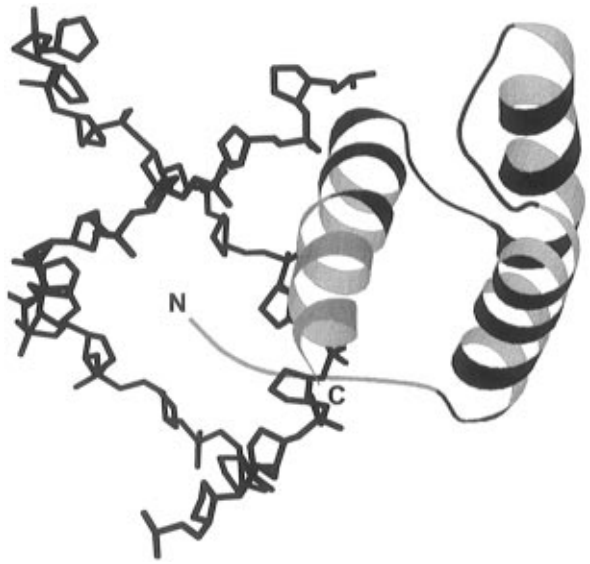

FIGURE 1: Ribbon drawing of the MATα2 homeodomain bound to DNA, made with the program Molscript (Kraulis, 1991), using coordinates from the Protein Data Bank (1apl.ent; Wolberger et al., 1991). Residues 4−9 and 50−58 are in gray and all others in black [numbering scheme of Wolberger et al. (1991)]. The DNA sugar-phosphate backbone is shown in black, and is from the consensus binding site.

The induction of increased or altered structure upon DNA binding has been found for many proteins (Spolar & Record, 1994; Reedstrom & Royer, 1995), including two homeodomains (Tsao et al., 1994, 1995; Cox et al., 1995). In

† This work was supported by ACS Grant IRG 11-35 to J.H.C. and NIH Grant GM 48036 to P.L.P.

* To whom correspondence should be addressed. Telephone: 410-516-6532. Fax: 410-516-5213.

⊗ Abstract published in *Advance ACS Abstracts,* January 1, 1997.

S0006-2960(96)02206-4 CCC: $14.00

these cases, the apparent energies of association of molecules include components from both the interaction of the protein with DNA and from the conformational change in the protein, as well as from any conformational changes in the DNA.

Thermodynamic studies of protein−DNA interactions provide a description of the forces which drive macromolecular complex formation and thus are complementary to structural studies. Understanding the energetics of DNA binding requires direct measurement of the changes in enthalpy, entropy, and heat capacity involved. These components of the Gibbs free energy changes of folding and association represent the fundamental forces which drive the processes and can be directly measured using the techniques of differential scanning (DSC)[1] and isothermal titration (ITC) calorimetry (Breslauer et al., 1992).

Other techniques, including electrophoretic band-shift assays, quantitative DNase footprinting assays, filter-binding assays, and fluorescence measurements, can be used to characterize the thermodynamics of DNA binding. However, these approaches do not directly measure energy changes and therefore are all ultimately inferential, as has been pointed out (Ladbury et al., 1994). In each of these techniques, the measured quantity is proportional to the population of bound and unbound species, from which the equilibrium constant of binding is determined. The enthalpy change of binding can then be found from the variation of the equilibrium with temperature, assuming the van't Hoff relationship holds. The heat capacity change of binding can in principle be found from the temperature derivative of ΔH; however, now one is taking the second derivative of the measured quantity, and large errors are unavoidable.

ITC is especially useful for measuring the enthalpy and heat capacity changes of protein−DNA association over the low-temperature range from 10 to 37 °C but has the disadvantage that the sensitivity of the instrumentation is inadequate to measure association constants of greater than about 10^8−10^9 M^{-1}, which includes many cases of sequence-specific DNA binding by proteins. Additionally, secondary processes occurring during titration with their own associated energies can be problematic. These may include protein oligomerization and aggregation or shifts in a mixed population of fully folded and unfolded protein molecules, the latter especially at the higher end of the temperature range.

While there are several examples of the application of ITC to protein−DNA association (Ladbury et al., 1994; Hyre & Spicer, 1995; Merabet & Ackers, 1995; Lundback & Hard, 1996), DSC has been relatively little used in the study of sequence-specific interactions. One disadvantage of DSC for this purpose is that the measured energy changes occur at higher temperatures and must be extrapolated back to the physiological range. Also, the melting of DNA and protein−DNA species can be complicated processes with multiple endotherms and second or third-order concentration dependencies. The advantages of DSC over ITC are that the Gibbs free energy change of binding for very strong associations can be measured (Brandts & Lin, 1990) and secondary processes avoided or taken into account. The necessary extrapolation to low temperatures is comparable to that commonly used and accepted in thermal denaturation studies of protein folding. We have therefore undertaken this study to determine the energetics of the α2 homeodomain interaction with DNA using both DSC and ITC, as a complement to existing structural and genetic information.

[1] Abbreviations: C_p, heat capacity; $\langle C_p \rangle$, excess heat capacity; T_m, melting temperature; T_T, transition temperature; CD, circular dichroism; TAPS, total association at partial saturation; DSC, differential scanning calorimetry; ITC, isothermal titration calorimetry.

EXPERIMENTAL PROCEDURES

(1) Protein Purification. The 128−210 amino acid fragment of the MATα2 protein containing the homeodomain was purified from overproducing *Escherichia coli* containing the plasmid pAV105, kindly provided by Martha Stark in the laboratory of Alexander Johnson. The bacteria were grown in TB broth (Sambrook et al., 1989) at 37 °C. One liter cultures were simultaneously inoculated with 1 mL of saturated overnight culture and induced with IPTG at 10^{-3} M. Purification was carried out essentially using the urea extraction method of Shortle and Meeker (1989) for staphylococcal nuclease, except that urea was removed by dialysis before the first chromatographic step, which was done using a Metachem Productiv-S cation exchange column. After elution from this column with a 200 mM NaCl step, the protein was dialyzed versus water, lyophilized, and further purified on a FPLC Mono-S column with a 0 to 1 M NaCl gradient in 10 mM Tris-HCl (pH 7.0) and 1 mM EDTA. The protein was again dialyzed versus water and lyophilized to a powder. Protein concentrations were determined using an A_{280} value of 1.43 cm^{-1} for a 1 mg/mL solution, calculated by the method of Gill and von Hippel (1989).

(2) DNA Preparation. DNA oligonucleotides were obtained from Biosynthesis Inc. They were purified over a FPLC Mono-Q column, using a 0 to 1 M NaCl gradient in 10 mM Tris-HCl (pH 7.0), 1 mM EDTA, and 20% acetonitrile. Extinction coefficients for each single strand were calculated from the sequence with nearest-neighbor effects using the program Oligo (Cantor & Warsaw, 1970; Rychlik & Rhoads, 1989). DNA sequence 1 was 5′-GCG CGA CAT GTA ATT CGC GCG, and sequence 2 was 5′-GCG CGA CAT TTA ATT CGC GCG. Complementary strands to these sequences were hybridized in equimolar concentrations before each experiment by heating to 100 °C for 1 min in the experimental buffer [20 mM sodium phosphate (pH 7.0), 1 mM EDTA, and varying NaCl concentrations], followed by slow cooling to room temperature. Complete hybridization of the strands was verified by sizing chromatography over a FPLC Superose-12 column in 10 mM sodium phosphate (pH 7.0), 1 mM EDTA, and 100 mM NaCl. A single sharp peak eluted off the column, indicating that the DNA was present in one homogeneous species.

(3) Protein−DNA Complex Formation. Protein and DNA samples were prepared by first dialyzing protein and duplex DNA individually, overnight at room temperature in the experimental buffer. After concentration measurement, the samples were diluted to 1.18 mg/mL for the protein (1.21×10^{-4} M) and 1.56 mg/mL for the DNA (1.21×10^{-4} M). Samples were prepared for calorimetry or CD by 2-fold dilution of the protein with buffer (to 0.56 mg/mL) and of the DNA with buffer (to 0.78 mg/mL) and addition of the protein solution in equal volume to the DNA solution. The concentrations of protein and DNA in the complex sample were thus made the same as the concentration of that component in its individual sample, within pipetting error.

(4) Differential Scanning Calorimetry. Scanning calorimetry was performed using a DSC-92 calorimeter built at

The Johns Hopkins University from a DASM-1 prototype. The cell volume was 1.3 mL and the scan rate 1 K/min. Buffers used were 20 mM glycine hydrochloride and 1 mM EDTA, from pH 3.5 to 5.0, and 20 mM sodium phosphate and 1 mM EDTA, from pH 6.0 to 7.0. The added NaCl concentration in the buffer is specified for each experiment. The partial specific heat capacity of the protein, DNA, and the protein−DNA complex was calculated (Privalov & Potekhin, 1986) using a MW for the homeodomain of 9748 and for the DNA of 12 854. The partial specific volume of the protein was calculated from the amino acid composition to be 0.744 $cm^3\ g^{-1}$ (Makhatadze et al., 1990). The PSV of the DNA was taken as 0.54 $cm^3\ g^{-1}$ (Durchslag, 1986). The PSV of the complex was taken to be 0.628 $cm^3\ g^{-1}$, an average of those of the protein and DNA, adjusted for their molecular weights.

Calorimetric data on the protein unfolding alone were analyzed using a two-state model with a temperature-dependent ΔC_p (Freire, 1994, 1995; Carra et al., 1996). The calorimetric enthalpy change of melting the DNA was determined by integrating the excess heat capacity after fitting to a four-state model. Data on the protein−DNA complexes and on the salt concentration dependence of protein unfolding were analyzed using models described in the Appendix. Nonlinear least-squares fitting was performed using equations input into the program NLREG (Phillip H. Sherrod, author).

(5) Isothermal Titration Calorimetry. ITC measurements were done on a MicroCal Omega 2 instrument at the Biocalorimetric Center at The Johns Hopkins University To determine the ΔH and ΔC_p of protein−DNA association, the homeodomain protein at 1.2×10^{-4} M was titrated in 15 μL injections into duplex DNA (sequence 1) at 6×10^{-5} M, under conditions of total association at partial saturation (TAPS). Three injections were made at each temperature and the results averaged. The standard deviation between injection heats was less than 6%. The heat of binding was corrected for the small endothermic heat of dilution of protein, which was found by injecting protein into buffer. Injection of buffer into DNA gave no measurable heat effect. The cell volume was 1.36 mL, and its contents were stirred at 400 rpm. The injection duration was 9 s. The equilibration time between injections was 3 min. For experiments titrating the DNA to saturation, protein at 1.2×10^{-4} M was titrated into DNA at 8.0×10^{-6} M, in 23 injections of 12 μL. Data were analyzed using Microcal's Origin program.

(6) Circular Dichroism and Fluorescence Measurements. Circular dichroism measurements were performed using a Jasco 710 spectropolarimeter with the PTC348 peltier temperature control accessory. The molar ellipticity of the protein was calculated using an average molecular weight per residue of 118.5. The ellipticity of the DNA and protein−DNA complexes was calculated in the same way, to facilitate comparison of spectra. CD melting experiments were analyzed by fitting to a two-state model (Carra et al., 1996) using a constant ΔC_p of 1 kJ K^{-1} mol^{-1}.

Digestion of the DNA in the protein−DNA complexes was accomplished using staphylococcal nuclease at 25 °C for 24 h. One hundred microliters of complex at 0.59 mg/mL protein and 0.78 mg/mL DNA was diluted into 300 μL of buffer [7 mM sodium phosphate (pH 7.0), 0.3 mM EDTA, 300 mM NaCl, and 30 mM $CaCl_2$], and SNase was added to 0.065 mg/mL. Digested DNA was removed by dialysis (3000 MW cutoff). The CD spectrum of SNase at 0.065 mg/mL was subtracted from the spectrum of the remaining protein.

Fluorescence measurements were done using an Aminco-Bowman fluorimeter with a water-jacketed cuvette holder for temperature control. Excitation of tryptophan was at 295 nm. The protein concentration was 0.118 mg/mL in a 1 cm cuvette.

Table 1: Thermodynamics of Unfolding of the MATα2 Homeodomain

pH	[NaCl][a]	[protein][b]	ΔH_{cal} [c]	ΔH_{fit} [d]	$\Delta H_{fit}/\Delta H_{cal}$	T_m [e]	ΔS [f]	σ^2 [g]
Calorimetric Results								
3.5	100	0.84	169	171	1.01	321.0	0.53	0.069
4.0	0	2.66	158	160	1.01	322.2	0.49	0.003
4.0	100	3.07	170	171	1.01	325.5	0.52	0.002
4.0	200	2.17	174	175	1.01	327.4	0.53	0.011
4.0	300	2.19	171	174	1.02	329.2	0.52	0.011
4.0	400	2.25	170	173	1.02	330.2	0.51	0.015
5.0	100	0.92	164	168	1.02	329.6	0.50	0.060
6.0	100	0.94	158	165	1.04	331.4	0.48	0.071
7.0	0	1.24	136	141	1.04	329.5	0.41	0.018
7.0	50	0.57	159	160	1.01	330.5	0.48	0.044
7.0	100	0.59	149	155	1.04	329.6	0.45	0.173
7.0	100	0.59	144	143	0.99	329.0	0.44	0.082
7.0	100	0.80	161	164	1.02	333.3	0.48	0.044
7.0	100	1.55	165	167	1.01	330.6	0.50	0.007
7.0	100	1.61	163	165	1.01	332.5	0.49	0.013
7.0	100	3.23	161	167	1.04	332.7	0.48	0.004
7.0	200	0.57	170	170	1.00	333.3	0.51	0.077
7.0	300	0.57	174	177	1.02	334.6	0.52	0.039
Circular Dichroism Results								
4.0	100	0.30		155		328.4	0.47	
7.0	0	0.26		178		330.0	0.54	

[a] The added NaCl concentration in millimolar. [b] The α2 homeodomain concentration in milligrams per milliliter. [c] The calorimetric enthalpy change of unfolding ΔH_{cal} in kilojoules per mol, obtained by integrating the area under the curve. Errors are ±10%. [d] The enthalpy change ΔH_{fit} calculated by fitting the data to a two-state model, in kilojoules per mole. [e] The melting temperature T_m in kelvin, where the transition is half complete, obtained from the fitting. Errors are ±1 K. [f] The enthalpy change of unfolding ΔS, in kilojoules per kelvin per mole. [g] The variance of the fit σ^2, in kilojoules per kelvin per mole.

RESULTS

Unfolding of the Protein in DSC. DSC experiments on the α2 homeodomain at various pHs and added NaCl concentrations revealed that unfolding of the protein is a two-state process (Table 1), meaning that intermediate states in unfolding are not significantly populated (Privalov, 1979). In Table 1, the ratio of the two state model fitted enthalpy change (ΔH_{fit}) to the calorimetric enthalpy change (ΔH_{cal}) is within a few percent of 1, consistent with the reaction of unfolding involving a monomeric protein molecule going from the folded to the unfolded state.

Reheating the sample after heating to 100 °C and cooling gives an endotherm with about 75% of the area of the first scan (not shown); therefore, the process is effectively reversible for calorimetry. At a lower pH (4.0 or 5.0), the reversibility is greater and the second scan almost coincident on the first. There is no significant protein concentration dependence of T_m over the range used. ΔH_{cal} is relatively small, around 160 kJ mol^{-1}. The absolute heat capacity of the protein itself at 15 °C is 20 ± 1 kJ K^{-1} mol^{-1}, high compared to that expected for a fully compact globular protein (Privalov, 1979), but this is largely due to the existence of unfolded N- and C-terminal tails in the native state solution structure. We estimate ΔC_p from the difference

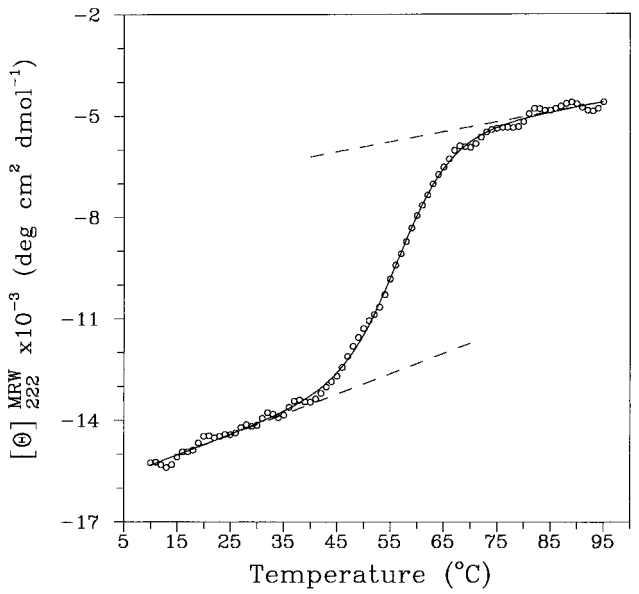

FIGURE 2: Melting of the α2 homeodomain at pH 7.0 with 0 mM NaCl, monitored by circular dichroism at 222 nm: (○) experimental data, (—) fitted curve, and (- - -) extrapolated ellipticities of the folded and unfolded states.

in extrapolated heat capacity between the unfolded and folded states at T_m to be 1 ± 1 kJ K^{-1} mol^{-1}. Determination of ΔC_p by variation of T_m with pH is not a viable alternative in this case, as ΔH_{cal} is relatively small and may be affected significantly by ionization enthalpies of side chains. The difference in ΔH upon variation of pH is within the 10% error of measurement for these fairly small enthalpy changes.

The T_m of the protein is reduced about 10 °C by decreasing the pH from 7.0 to 3.5. Adding NaCl to 400 mM increases T_m by several degrees, which is not surprising as the homeodomain is a strongly charged molecule, with a calculated net charge of +8 at pH 7.0. Unfavorable electrostatics in the more densely packed folded state would be compensated for by an increase in ionic strength and protein folding thereby favored. If we interpret this effect as discrete binding of NaCl to the folded form of the protein, the data at pH 4.0 and varying salt concentrations can be globally analyzed with a linkage equation (see the Appendix) to yield a NaCl binding stoichiometry to the folded state of 1.1, with a K_D of 0.16 M.

Denaturation Probed by Spectroscopic Methods. Unfolding of the protein can also be followed by circular dichroism (Figure 2). The values obtained for T_m and ΔH are in reasonable agreement with those from calorimetry (Table 1). Although there is a temperature dependence of the native state ellipticity in Figure 2, no additional cooperative folding transitions at low temperatures can be detected by CD, and wavelength spectra taken at 5 °C reveal no increase in α-helical content upon cooling from 25 °C (not shown). This indicates that there is not an increase in folding at low temperatures which would need to be taken into consideration in calculating the energetics of the protein.

The homeodomain contains two tryptophans whose fluorescence can also be used to probe structure. One of these is in the DNA recognition helix and is highly conserved among homeodomains (Wolberger, 1993). Upon heating from 26 to 58 °C, the intensity of fluorescence from the protein increases, while the wavelength of maximal emission is red-shifted (not shown). Fluorescence in the folded state is quenched relative to that of the unfolded state, presumably due to interactions of the tryptophans with other residues in the structure. The observed fluorescence intensity of the homeodomain is maximal near the protein's T_m, because at T_m the population of unfolded protein is increasing most rapidly. Upon further heating, the intensity decreases due to the steep intrinsic temperature dependence of tryptophan fluorescence.

Sequence and Stability of the DNA Site. To examine the binding of the α2 homeodomain to DNA, we prepared a 21-base pair sequence containing a consensus binding site (Wolberger et al., 1991) for α2 (DNA sequence 1):

```
      1          10          21
5′-GCG CGA CAT GTA ATT CGC GCG

3′-CGC GCT GTA CAT TAA GCG CGC
```

Positions 6−16 contain the binding site and are flanked on each side by five G·C base pairs. These flanking sequences were added to increase the stability of the DNA so that under some conditions the protein in a protein−DNA complex would melt before the DNA does. Also, potential effects on affinity of the protein being at the very end of the DNA molecule are thus avoided.

In Figure 3, DSC curves are presented for melting of the protein alone, the DNA alone, and the protein−DNA complex, at pH 7.0 and various NaCl concentrations. The stability of the DNA increases with increasing salt concentrations, due to electrostatic interactions with the densely charged phosphate backbone. Scans on the DNA show a broad early shoulder before a sharper transition and are virtually 100% reproducible on repeated heating. Strand dissociation occurs in the later region of the endotherm, judging by its sharpness.

Melting of the Protein−DNA Complexes. The shapes of the curves for melting of the protein−DNA complexes in Figure 3 change with variation of the salt concentration. The excess heat capacity separates out into two peaks when NaCl is increased from 0 to 200 mM [over 20 mM sodium phosphate (pH 7.0) and 1 mM EDTA sodium salt]. The latter peak at 50, 100, and 200 mM NaCl closely parallels the curve for the DNA alone under the same conditions. For these cases, melting of the DNA in the complex follows dissociation and unfolding of the protein, which represents the earlier half of the scans on the complexes. The curves for melting the complexes are mostly but not entirely reproducible on reheating, as are the curves for the protein alone.

The two heat capacity peaks diverge as the NaCl concentration is increased because salt produces opposing effects, increasing the stability of the duplex DNA while weakening the interaction between the protein and DNA. At 0 mM added NaCl, the relative stability of the complex is greater than that of its DNA component, so unfolding of the DNA and protein occurs together in one very sharp peak. Table 2 gives values for the total enthalpy changes of melting of the complexes.

Detailed analysis of the entire process of melting the protein−DNA species requires some simplification, which we have approached by separation of the reaction into stages involving first the dissociation and unfolding of the protein and then the melting of the DNA. By subtracting the heat capacity function of melting the DNA from the heat capacity of melting the protein−DNA complex, we can effectively remove the contribution of denaturation of the DNA from

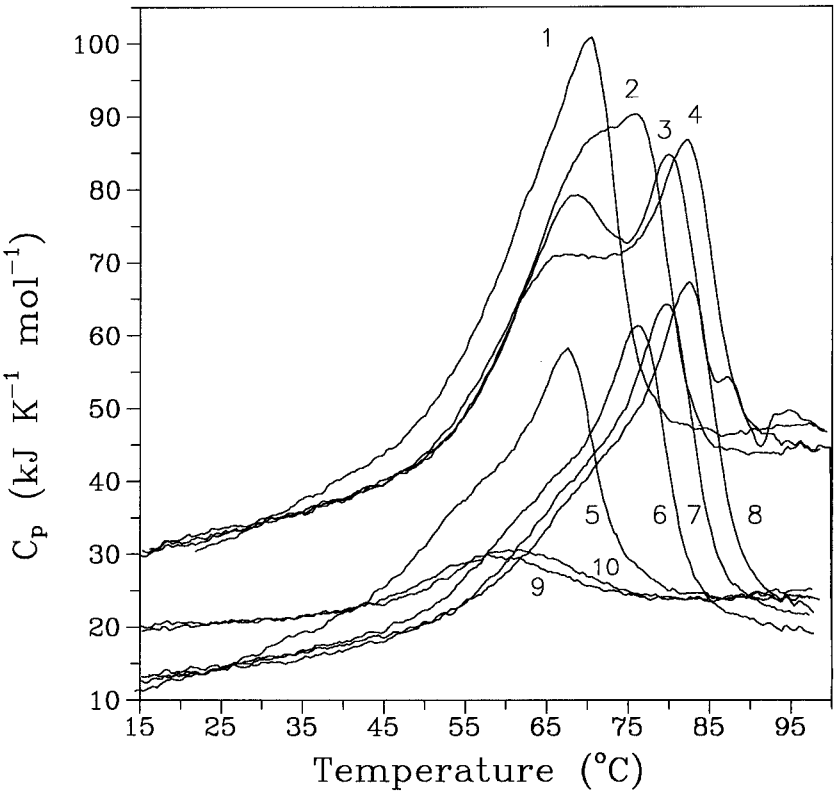

FIGURE 3: Calorimetry on the α2 homeodomain, DNA (sequence 1, see text), and the protein−DNA complex, at pH 7.0 and various salt concentrations: (1) protein−DNA, 0 mM NaCl; (2) protein−DNA, 50 mM NaCl; (3) protein−DNA, 100 mM NaCl; (4) protein−DNA, 200 mM NaCl; (5) DNA, 0 mM NaCl; (6) DNA, 50 mM NaCl; (7) DNA, 100 mM NaCl; (8) DNA, 200 mM NaCl; (9) protein, 50 mM NaCl; and (10) protein, 200 mM NaCl.

Table 2: Melting of the DNA Sequence 1 and Protein−DNA Complexes

[NaCl][a]	ΔH_{DNA}[b]	ΔH_{comp}[c]	$\Delta H_{comp-DNA}$[d]	$\Delta H_{diff-Cp}$[e]	ΔH_D (25°C) [f]	K_D (25°C)[g]	σ^2 [h]
0	734	1112	378				
50	804	1124	320	334	74	1.5×10^{-8}	0.358
100	839	1143	304	315	81	4.0×10^{-8}	0.466
200	855	1161	306	305	54	5.0×10^{-7}	0.051
300	854	1080	226	271	25	1.3×10^{-5}	0.061

[a] The added NaCl concentration in millimolar. [b] The calorimetric enthalpy change ΔH_{DNA} of unfolding a duplex DNA at pH 7.0, in kilojoules per mole. Errors are ±10%. [c] The calorimetric enthalpy change ΔH_{comp} of unfolding a protein/DNA mixture at pH 7.0, in kilojoules per mole. Errors are ±10%. [d] The difference in calorimetric enthalpies $\Delta H_{comp-DNA}$ between the protein/DNA mixture and the DNA alone, in kilojoules per mole. [e] The enthalpy change ΔH_{diff-C_p} in kilojoules per mole derived by integrating the difference heat capacity curves, which were obtained by subtracting the DNA heat capacity function from the protein−DNA complex heat capacity function. [f] The calculated enthalpy change ΔH_D of dissociation of the protein−DNA complex at 25 °C, in kilojoules per mole. [g] The calculated dissociation constant K_D of the protein−DNA complex at 25 °C, in molar. [h] The variance of the fit of the difference heat capacity curves σ^2, in kilojoules per kelvin per mole.

the reaction. Because the excess heat capacity function is not a state function, this approach will be valid only if the reaction of melting the DNA is essentially independent of melting the protein, which appears to be more or less true at NaCl concentrations of 50 mM and greater. Thus, the reaction of unfolding the complex is considered to be

$$\begin{array}{ccc} P_FD & \Longleftrightarrow & P_F + D \\ \Updownarrow & & \\ P_U + D & \Longleftrightarrow & P_U + S_A + S_B \end{array}$$

where D is duplex DNA, S_A and S_B are single strands, P_F is the folded protein, and P_U is the unfolded protein.

Following this rationale, in Figure 4A, we have normalized the heat capacity functions of the protein, DNA, and protein−DNA species at 50 mM NaCl to zero at 15 °C. The curve for the DNA was then subtracted from the protein−DNA curve to yield a difference heat capacity curve representing the protein component of the complex. This was also performed for the curves at 100, 200, and 300 mM NaCl, yielding the difference curves shown in Figure 4B. As the salt concentration is increased, the total enthalpy in the difference curve decreases, along with the temperature of the maximum heat capacity. For the data at 0 mM NaCl, this approach is not applicable due to the mainly concerted nature of the protein and DNA unfolding, and we do not present the difference curve.

Simulation of the difference curves allowed determination of ΔH_D, the enthalpy change of protein−DNA dissociation, and K_D, the dissociation constant. Essentially, the increase in enthalpy content and stability due to complex formation is represented by the difference curve versus the corresponding scan on the protein alone (Figure 4A). The data were analyzed using a model (Brandts & Lin, 1990) which takes into account the existence of three species: folded protein bound to DNA and unfolded and folded protein free of DNA. Data for melting of the protein alone at each salt concentration and known ΔC_p values for the association (discussed

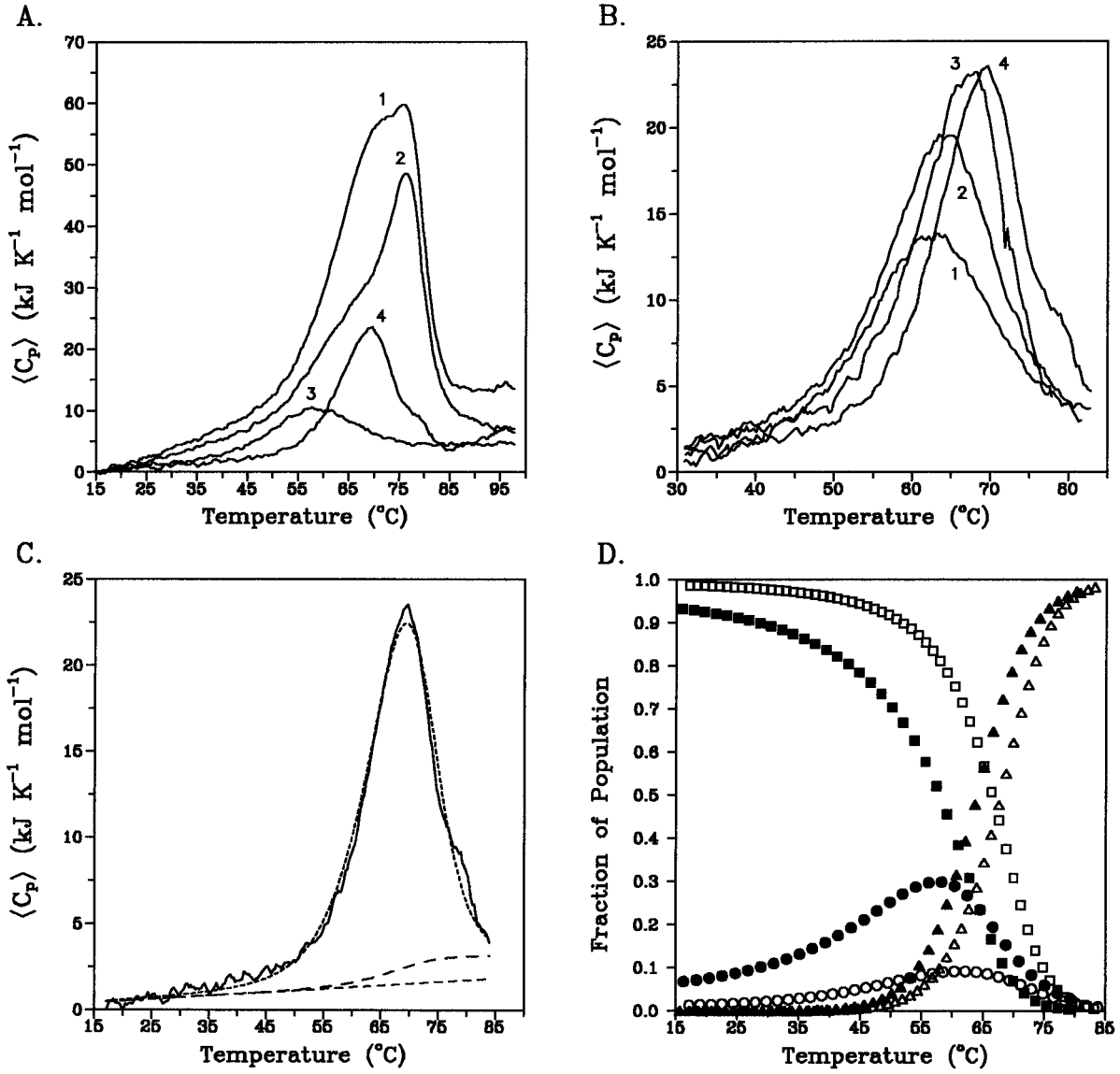

FIGURE 4: (A) Excess heat capacities at pH 7.0 with 50 mM NaCl. For each case, the heat capacity has been normalized to zero at 15 °C: (1) the protein−DNA (sequence 1) complex; (2) the DNA, (3) the α2 homeodomain protein, and (4) the difference heat capacity function of the complex minus the DNA (curve 1 minus curve 2). (B) Difference heat capacity functions, as in part A: (1) 300 mM NaCl, (2) 200 mM NaCl, (3) 100 mM NaCl, and (4) 50 mM NaCl. (C) The difference heat capacity function at 50 mM NaCl simulated as described in the Appendix: (—) the data, (- - -) the fitted curve, (— — —) the extrapolated pretransitional heat capacity, and (— — —) the baseline heat capacity taken in proportion to the completion of unfolding. (D) The populations of species extant during unfolding of the protein−DNA complex at 50 and 200 mM NaCl, in terms of the fraction of total protein: (■) the complex at 200 mM NaCl, (●) folded unbound protein at 200 mM NaCl, (▲) unfolded protein at 200 mM NaCl, (□) the complex at 50 mM NaCl, (○) folded unbound protein at 50 mM NaCl, (△) unfolded protein at 50 mM NaCl.

below) and unfolding reactions were used in the analysis (see the Appendix).

Figure 4C shows the result of this simulation for the data at 50 mM NaCl. The model is able to fit the process well, judging by the agreement of simulation and data. Table 2 gives values for the enthalpy change ΔH_D and dissociation constant K_D at 25 °C. The population of each species can be calculated from the simulation. These are shown in Figure 4D for the experiments at 50 and 200 mM NaCl. At 50 mM NaCl, the population of folded unbound protein is never greater than 9%, but at 200 mM NaCl, it maximally reaches 30%. At 300 mM NaCl (not shown), the interaction of the protein and DNA is weakened such that 34% of the protein is initially present in the unbound folded form, and this fraction reaches 59% maximally. Errors on these calculations are small near the measured melting temperatures but increase with extrapolation across the temperature range.

The total observed enthalpy difference of melting the protein/DNA mixture versus the DNA alone can be found either by integrating the difference heat capacity functions of Figure 4C ($\Delta H_{\text{diff}-C_p}$, Table 2) or by subtracting the total calorimetric enthalpies for each case (leaving $\Delta H_{\text{comp}-\text{DNA}}$). We say the protein/DNA mixture because at the higher salt concentrations not all of the protein is initially present in complex with the DNA. The numbers obtained by the two methods agree reasonably well. Both $\Delta H_{\text{comp}-\text{DNA}}$ and $\Delta H_{\text{diff}-C_p}$ are smaller at 300 mM NaCl than at the lower salt concentrations, because in this case about one-third of the protein is unbound initially.

ITC Measurements of Binding. We also measured the enthalpy of protein−DNA association using isothermal titration calorimetry. The enthalpy of binding in 100 mM NaCl at 25 °C was found to be -90.5 ± 6 kJ mol^{-1}, within 10% of the value from DSC (-81 kJ mol^{-1}, Table 2).

Titration of the DNA (sequence 1) with protein at varying temperatures allowed determination of ΔH_D as a function of temperature. Linear regression of this data yielded ΔC_{pA}, the apparent heat capacity change of association, which was -2.2 ± 0.2 kJ K^{-1} mol^{-1}. It should be noted that this figure includes contributions from conformational changes in the protein occurring as it binds DNA and is not only due to the interaction of fixed structures. DSC scans on the DNA at 100 mM NaCl show that it is completely folded over the temperature range used in ITC (Figure 3).

From the absolute heat capacities of the protein, DNA, and protein−DNA species measured by DSC, the difference between the C_p of the complex and the sum of its components amounts to -2 to -3 kJ K^{-1} mol^{-1} at 20 °C, consistent with the number determined more accurately by ITC. The apparent ΔC_{pA} value of -2.2 kJ K^{-1} mol^{-1} was used in fitting the DSC data on melting of the complexes, as discussed above.

ITC experiments in which protein was added to the DNA until saturation yielded heats for the initial injections that were equal to those measured using total association at partial saturation. However, after saturation of the primary binding mode of the DNA, exothermic heats of addition of protein were still observed (data not shown). These continuing injection heats were about 35% of the initial heats after apparent completion of the primary binding mode but gradually decreased with further injections. They were not identifiable with the heat of dilution, which was independently measured and found to be 7% of the initial binding heat in absolute magnitude and endothermic. These continuing heats probably represent an aggregation of more protein onto the 1:1 complex, which was observed as two or more additional bound species in electrophoretic band-shift assays (not shown). For this reason, the K_D of binding could not be reliably determined from ITC.

CD Spectrum of the Protein-DNA Complex. A comparison of circular dichroism spectra of the protein, DNA, and protein−DNA species reveals a significant conformational change in the protein on binding (Figure 5). Subtraction of the DNA component from the protein−DNA CD spectrum leaves a difference spectrum having 20% more ellipticity at 220 nm than the protein alone. The shape of the difference CD curve indicates the formation of more α-helical structure in the protein upon complex formation. An increase of ellipticity at 220 nm of 20% is consistent with helix formation in about six residues of the C-terminal half of the recognition helix.

The largest increase in ellipticity in the difference spectrum lies at 216 nm, where the ellipticity of the DNA is zero. This fact, and the observation that the DNA in the α2/DNA cocrystal structure is essentially B-form (Wolberger et al., 1991), supports the assignment of the conformational change to the protein and not the DNA component of the complex. After digestion of the DNA in the complex with a nuclease, the CD spectrum of the protein returned to the shape observed before addition of DNA (not shown). The additional folding induced by DNA is therefore reversible.

NonSpecific Binding. We also studied the interaction of the α2 homeodomain with another DNA sequence in which the G at position 10 (see above), conserved among α2 binding sites, was changed to T (DNA sequence 2). This change was incorporated to reduce the affinity of the α2 homeodomain for the DNA, creating a non- or semispecific binding site. With this sequence, the difference CD spectrum

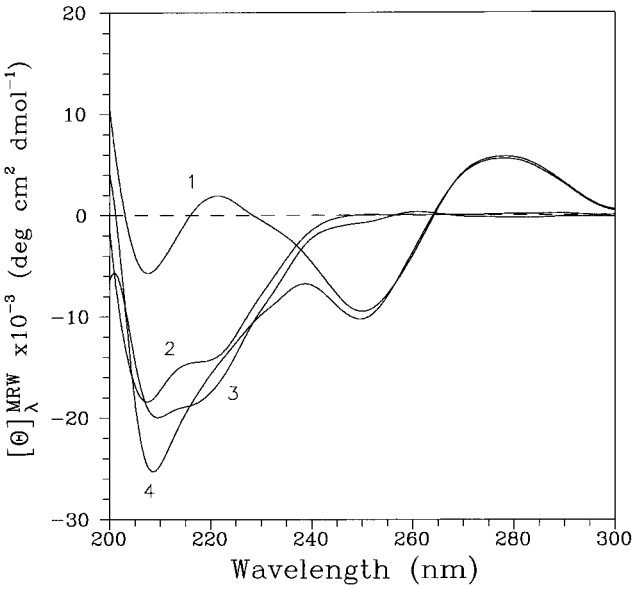

FIGURE 5: Circular dichroism spectra at pH 7.0, 50 mm NaCl, and 25 °C. Units for the protein are degrees per cm^2 per decimole of amino acid residues, calculated using an average MW of 118.5. The ellipticity of the DNA was calculated using the same figure in order to show the relative magnitudes of the protein and DNA signals. The units for the DNA ellipticity are therefore merely arbitrary: (1) the DNA (sequence 1) at 0.75 mg/mL, (2) the α2 homeodomain at 0.57 mg/mL, (3) the difference spectrum of curve 4 (P−DNA complex) minus curve 1 (DNA), and (4) the protein−DNA complex, with components at the above concentrations.

(not shown) had the shape of that of the free protein, indicating no increase in secondary structure. DSC measurements revealed no detectable association of the protein and DNA, judging by the enthalpy content of the complex compared to that of the free components (not shown). The association we are measuring by CD and scanning calorimetry is therefore sequence-specific.

DISCUSSION

Energetics of the DNA-Binding Reaction from DSC and ITC

Brandts and Lin (1990) pointed out the utility of DSC for the study of very tight macromolecular interactions, yet little detailed analysis of sequence-specific protein−DNA complexes by DSC has since been done, perhaps because of the complicated nature of the unfolding processes involved. Herein, we have attempted to deal with these complications by using solution conditions and a DNA sequence such that the DNA melts largely after the protein does; thus, the melting of the DNA can be considered an independent reaction subtractable from the overall process. Unfolding of protein in the protein−DNA complex contributes to the DSC scan both the intrinsic ΔH of unfolding the free protein from its solution conformation and the enthalpy of dissociation ΔH_D. However, the observed enthalpy change upon heating the protein/DNA mixture includes some contribution from melting the protein free in solution as well as in the complex. It is therefore necessary to find ΔH_D and K_D by simulating the whole process of melting the mixture of species (Table 2). Association of the homeodomain with DNA is enthalpically driven throughout the entire physiological temperature range, while the entropy change is unfavorable to binding.

The dissociation constant K_D was found to be 1.5×10^{-8} M at 50 mM NaCl and increased with the salt concentration,

reflecting the weakening of electrostatic interactions between the protein and DNA. From 200 to 300 mM NaCl, K_D changes by a factor of 300, which does not agree with the trend of the other salt concentrations. This abrupt change is not likely to be real and instead probably reflects an inherent weakness of the DSC method for determining the energies of interactions when association is too weak and the initial population is not entirely in the ligated species. The values of K_D and ΔH_D at 300 mM NaCl are therefore unreliable and should be discounted. We would estimate the error on the other K_D values to be approximately 2-fold and the error on ΔH_D at 25 °C calculated from DSC data to be ± 15 kJ mol^{-1}.

The agreement of ΔH_D values determined by DSC and ITC is a strong argument for the validity of the analysis of difference heat capacity functions. The overlap of the early heat capacity shoulder of the DNA with the melting of protein from the protein−DNA species is neglected with justification. The symmetry of the difference curves of Figure 4C supports the contention that melting of the protein can be considered independently of the early DNA shoulder, which detailed analysis (not shown) reveals contains at least two endothermic transitions. If the early changes in the DNA were linked to the protein dissociation reaction, then the presence of protein in the complex would shift the excess heat capacity of the early DNA transitions to higher temperatures. The result would be a negative slope in the difference heat capacity functions ($\langle\langle C_p\rangle$ of the complex minus $\langle C_p\rangle$ of the DNA) in the low-temperature region, which was not observed (Figure 4C). Therefore, the low-temperature endotherms of the DNA appear to be unlinked to protein binding. We suspect the early endotherms of the DNA represent partial unfolding of the duplex from its ends, before the majority of secondary structure loss and strand dissociation occurs. As the ends of the DNA are separated by several base pairs from the sequence recognized by the homeodomain, the early transitions may not affect the bound protein appreciably.

Deconvolution of the DNA-melting endotherms (not shown) revealed three endotherms, the last of which involves strand dissociation and must be linked to protein binding. The latter half of the protein-melting endotherm does partially overlap the third transition of the DNA at 50 mM NaCl, but this overlap decreases at higher salt concentrations because of the increasing separation of melting processes, as discussed below. To whatever extent the assumption of independence of protein and DNA melting processes is not true, the values of K_D obtained will be affected, but this error is not likely to be greater than the estimated 2-fold error of measurement on K_D.

Titration calorimetry was used to determine the heat capacity change of protein−DNA binding accurately, and this figure was then applied to analysis of the DSC data. ITC also provided an independent measurement of the enthalpy change of binding at 25 °C. The K_D of binding was not measurable by ITC because of nonspecific binding of protein to DNA after 1:1 saturation. However, because only stoichiometric quantities of protein and DNA were needed in DSC, unwanted nonspecific binding was avoided and both K_D and ΔH_D were measurable. A weak secondary binding mode was observed in an ITC study of *trp* repressor binding to DNA (Ladbury et al., 1994), but in that case, its contribution could be subtracted from the total reaction.

Effects of Salt on the Melting of the Homeodomain Complex

In Figure 3, an increase of the salt concentration causes the excess heat capacity of melting the protein/DNA mixture to divide into two discernible peaks. The effects of salt on the energetics of this process can be separated into three components.

(1) Stabilization of the Protein Structure. Addition of NaCl to 300 mM increases the T_m of the protein by about 5 °C, a small but significant contribution to the energies of the complex and of the folded protein in solution.

(2) Stabilization of the DNA Duplex. The temperature of the maximum excess heat capacity of the DNA increases by 16.6 °C on change of the added NaCl concentration from 0 to 300 mM. This is attributable to counterions interacting with the phosphate backbone.

(3) Destabilization of the Protein−DNA Interaction. The electrostatic component of interaction between the protein and DNA is weakened by increasing the ionic strength.

The net effect of increasing salt is therefore an increase in the separation of the processes of melting the DNA and dissociation/unfolding of the protein in the complex. The salt dependence of the protein−DNA interaction is expected to be entropic in origin, largely because of the release of bound cations from DNA, although our data are not extensive enough to test this assumption. In the absence of added salt beyond the 20 mM sodium phosphate in the buffer, the relative stabilities of components and their interaction is such that melting of the protein and DNA in the complex occurs largely together (Figure 3). In this case, the melting of the DNA is not an independent process and a different model for analysis of the data would be needed, which would have to take into account the ΔC_p and ΔH of unfolding the DNA itself, as well as a third-order concentration dependence.

Fluorescence of the Protein

Fluorescence was found to be quenched in the folded state relative to the unfolded state. Because of the complex temperature dependence of the fluorescence intensity, it was not possible to determine the thermodynamics of protein folding by this method. The identity of the particular interactions which quench fluorescence in the native structure, especially from the highly conserved tryptophan in the recognition helix, is an interesting question as yet unanswered. Native state quenching is also found for *trp* aporepressor and some other proteins (Royer, 1993).

Conformational Changes on Association

Using NMR spectroscopy, Phillips et al. (1991) assigned the secondary structure of the α2 homeodomain in solution. These authors found that helical structure in the C-terminal half of helix 3, from serine 50 to glutamate 56 [numbering scheme of Wolberger et al. (1991)], is present but significantly weaker than in the first half of the helix, on the basis of faster-exchanging amide protons and missing helical NOE connectivities. In contrast, the X-ray crystal structure of α2 bound to DNA (Wolberger et al., 1991; Li et al., 1996) shows helix 3 extending clearly to threonine 58. We find from circular dichroism measurements that the α-helicity of the α2 homeodomain increases by about 20% from its initial value upon DNA binding.

For two other homeodomains, NK-2 and Oct-1, structure in the latter half of helix 3 was shown to be induced by DNA binding, in these cases using a combination of NMR and X-ray crystallography (Tsao et al., 1994, 1995; Cox et al., 1995). We infer then from our results that residues 50−58 of the α2 homeodomain are substantially disordered in the free protein under the conditions used and in Figure 1 have colored them gray to indicate that structure is induced by DNA association. The relatively weak structure detected in the latter half of helix 3 by NMR in the study of Phillips et al. (1991) may contribute to the free protein's CD spectrum measured here, making the increase in ellipticity observed upon DNA binding more consistent with fully folding six rather than nine residues. Circular dichroism difference spectra were earlier found to be evidence for DNA-induced folding of the leucine zipper proteins GCN4, Fos, and Jun (Patel et al., 1990; Weiss et al., 1990).

Spolar and Record (1994) have analyzed data for several proteins having altered or increased structure upon DNA binding and found that the induced structure makes a significant contribution to the thermodynamics of association. The values which we obtain for the Gibbs free energy, enthalpy, and heat capacity changes of association of the α2 homeodomain should therefore be interpreted as including some contribution from conformational changes in the protein, as well as the intrinsic energy of the protein−DNA interface. Experimental decomposition of the energetic contributions to association from this induced structure would give insight into both protein folding and protein−DNA interactions.

ACKNOWLEDGMENT

We thank Martha Stark for providing a plasmid expressing the homeodomain and Craig Johnson for help with the ITC.

APPENDIX

(1) Global Fitting of the Salt Dependence of Protein Unfolding. Five curves for unfolding the MATα2 homeodomain at pH 4.0 in 20 mM glycine hydrochloride, 1 mM EDTA, and 0, 100, 200, 300, and 400 mM NaCl were first fitted individually to a two-state unfolding model (Freire, 1994, 1995; Carra et al., 1996) to obtain parameters characteristic of each transition. Then the curves were fit simultaneously to a model in which the equilibrium constant of unfolding K_U is influenced by the presence of the ligand NaCl present at a concentration of [L] (Ramsay & Freire, 1990).

$$K_U = K_0 \frac{1}{(1 + K_L(L])^N} \quad (1)$$

The ligand is assumed not to bind to the unfolded state and its free concentration to be effectively equal to its total concentration. K_0 is the unfolding equilibrium constant in the absence of ligand, and K_L is the binding constant of the ligand for the protein at each of N equivalent sites. The experiments were linked by a common enthalpy function based on the reference enthalpy change observed at the T_m found in 400 mM NaCl, with a constant ΔC_p of 1 kJ K^{-1} mol^{-1}.

(2) DSC Analysis of the Protein−DNA Complex Melting. Equations were adapted from those presented by Brandts and Lin (1990) for the case of a protein−ligand system with a 1:1 stoichiometry and a single unfolding transition. To analyze the melting of a protein−DNA complex, the heat capacity function of melting the DNA alone was subtracted from the heat capacity of melting the complex, after normalizing both to zero at 15 °C. This difference heat capacity function represents the endotherm of dissociation of the protein from the DNA together with protein unfolding. It is assumed that the presence of the bound protein does not appreciably affect the shape of the DNA melting curve, which may be true when the stability of the DNA is greater than that of the complex.

The melting of complexes at 50, 100, 200, and 300 mM NaCl was analyzed, using in each case the T_m of the protein under the same conditions as a reference temperature T_{T0} (Table 1). P_F is folded protein. P_U is unfolded protein. P_T is the total protein. D is free duplex DNA. $[D_T]$ is the total molar duplex DNA concentration. S_A and S_B are single DNA strands. It is assumed that only folded protein and double-stranded DNA can interact. ΔH_{U0} is the enthalpy change of unfolding the protein at T_{T0}. ΔH_{A0} is the enthalpy change and ΔG_{A0} the Gibbs free energy change of association of the protein and DNA at T_{T0}. ΔC_{p_U} for unfolding the protein was taken as 1 kJ K^{-1} mol^{-1} and ΔC_{p_A} for binding of the protein to DNA as −2.2 kJ K^{-1} mol^{-1}. ΔG_A is the free energy of association of the protein and DNA, while ΔG_{A*} represents its variation as a function of temperature. K_{A0} is the association constant at T_{T0} and is a fitted parameter, as is ΔH_{A0}.

The mass conservation equations for the total protein and DNA concentrations can be combined with the equilibrium constants of protein unfolding and protein−DNA association as follows:

$$[P_T] = [P_F] + [P_U] + [PD] = [P_F] + K_U[P_F] + K_A[D][P_F] \quad (2)$$

$$[D_T] = [D] + [PD] = [D] + K_A[D][P_F] \quad (3)$$

The enthalpy and heat capacity changes are used to define the Gibbs free energies of folding and association as functions of temperature:

$$\Delta H_A = \Delta H_{A0} + (T - T_{T0})\Delta C_{pA} \quad (4)$$

$$\Delta H_U = \Delta H_{U0} + (T - T_{T0})\Delta C_{pU} \quad (5)$$

$$\Delta G_U = \frac{T_{T0} - T}{T_{T0}}\Delta H_{U0} + (T - T_{T0})\Delta C_{pU} + T\Delta C_{pU} \ln(T_{T0}/T) \quad (6)$$

$$\Delta G_{A*} = \frac{T_{T0} - T}{T_{T0}}\Delta H_{A0} + (T - T_{T0})\Delta C_{pA} + T\Delta C_{pA} \ln(T_{T0}/T) \quad (7)$$

$$K_A = K_{A0} \exp\left(\frac{-\Delta G_{A*}}{RT}\right) \quad (8)$$

$$K_U = \exp\left(\frac{-\Delta G_U}{RT}\right) \quad (9)$$

The free DNA concentration can be found by solving a

quadratic equation:

$$[D] = \frac{-B + \sqrt{(B^2 - 4K_A C)}}{2K_A} \quad (10)$$

$$B = 1 + K_U + K_A([P_T] - [D_T]) \quad (11)$$

$$C = -[D_T](1 + K_U) \quad (12)$$

The relevant populations of species in the reaction can then be calculated as functions of temperature:

$$[P_F] = \frac{[P_T]}{1 + K_U + K_A[D]} \quad (13)$$

$$[PD] = \frac{[P_T]K_A[D]}{1 + K_U + K_A[D]} \quad (14)$$

$$[P_U] = \frac{[P_T]K_U}{1 + K_U + K_A[D]} \quad (15)$$

An excess enthalpy function $\langle H \rangle$, relative to the protein−DNA complex as reference state, can be written as follows:

$$\langle H \rangle = \Delta H_U \frac{[P_U]}{[P_T]} - \Delta H_A \frac{[P_F] + [P_U]}{[P_T]} \quad (16)$$

The excess heat capacity $\langle C_p \rangle$ as a function of temperature was found by numerical differentiation of $\langle H \rangle$. In simulation of the difference heat capacity functions, the pretransitional heat capacity of the complex was fitted as a linear function of temperature. The difference heat capacity after the endotherm of protein dissociation and unfolding was erratic; therefore, the data were truncated at the end of the peak for analysis.

REFERENCES

Baxter, S. M., Gontrum, D. M., Phillips, C. L., Roth, A. F., & Dahlquist, F. W. (1994) *Biochemistry 33*, 15309−15320.

Brandts, J. F., & Lin, L. N. (1990) *Biochemistry 29*, 6927−6940.

Cantor, C., & Warsaw, M. (1970) *Biopolymers 9*, 1059−1077.

Carra, J. H., Murphy, E. C., & Privalov, P. L. (1996) *Biophys. J. 71*, 1994−2001.

Clarke, N. D., Kissinger, C. R., Desjarlais, J., Gilliland, G. L., & Pabo, C. O. (1994) *Protein Sci. 3*, 1779−1787.

Cox, M., van Tilborg, P. J. A., de Laat, W., Boelans, R., van Leeuwen, H. C., van der Vliet, P. C., & Kaptein, R. (1995) *J. Biomol. NMR 5*, 23−32.

Durchslag, H. (1986) in *Thermodynamic Data for Biochemistry and Biotechnology* (Hinz, H.-J., Ed.) Springer-Verlag, Berlin, FRG.

Freire, E. (1994) *Methods Enzmol. 240*, 502−568.

Freire, E. (1995) *Annu. Rev. Biophys. Biomol. Struct. 24*, 141−165.

Gehring, W. J., Affolter, M., & Burglin, T. (1994) *Annu. Rev. Biochem. 63*, 487−526.

Gill, S. C., & von Hippel, P. H. (1989) *Anal. Biochem. 182*, 319−326.

Goutte, C., & Johnson, A. D. (1993) *J. Mol. Biol. 233*, 359−371.

Griko, Y., Freire, E., Privalov, G., Van Dael, H., & Privalov, P. (1995) *J. Mol. Biol. 252*, 447−459.

Hirsch, J. A., & Aggarwal, A. K. (1995) *EMBO J. 14*, 6280−6291.

Hyre, D., & Spicer, L. D. (1995) *Biochemistry 34*, 3212−3221.

Kamps, M. P., Murre, C., Sun, X., & Baltimore, D. (1990) *Cell 60*, 547−555.

Kissinger, C. R., Liu, B., Martin-Blanco, E., Kornberg, T. B., & Pabo, C. R. (1990) *Cell 63*, 579−590.

Kraulis, P. (1991) *J. Appl. Crystallogr. 24*, 946−950.

Ladbury, J. E., Wright, J. G., Sturtevant, J. M., & Sigler, P. B. (1994) *J. Mol. Biol. 238*, 669−681.

Li, T., Stark, M. R., Johnson, A. D., & Wolberger, C. (1995) *Science 270*, 262−269.

Lundback, T., & Hard, T. (1996) *Proc. Natl. Acad. Sci. U.S.A. 93*, 4754−4759.

Makhatadze, G., & Privalov, P. (1990) *J. Mol. Biol. 213*, 385−391.

Makhatadze, G., & Privalov, P. (1995) *Adv. Protein Chem. 47*, 307−425.

Makhatadze, G., Medvedkin, V., & Privalov, P. (1990) *Biopolymers 30*, 1001−1010.

Merabet, E., & Ackers, G. K. (1995) *Biochemistry 34*, 8554−8563.

Patel, L., Abate, C., & Curran, T. (1990) *Nature 347*, 572−575.

Phillips, C. L., Vershon, A. K., Johnson, A. D., & Dahlquist, F. W. (1991) *Genes Dev. 5*, 764−772.

Phillips, C. L., Stark, M. R., Johnson, A. D., & Dahlquist, F. W. (1994) *Biochemistry 33*, 9294−9302.

Privalov, P. L. (1979) *Adv. Protein Chem. 33*, 167−241.

Privalov, P. L., & Potekhin, S. A. (1986) *Methods Enzymol. 131*, 4−51.

Qian, Y. Q., Billeter, M., Otting, G., Muller, M., Gehring, W. J., & Wuthrich, K. (1989) *Cell 59*, 573−580.

Qian, Y. Q., Furukubo-Tokunaga, K., Resendez-Perez, D., Muller, M., Gehring, W., & Wuthrich, K. (1994) *J. Mol. Biol. 238*, 333−345.

Ramsay, G., & Freire, E. (1990) *Biochemistry 29*, 8677−8683.

Reedstrom, R., & Royer, C. (1995) *J. Mol. Biol. 253*, 266−276.

Royer, C. A., Mann, C. J., & Matthews, C. R. (1993) *Protein Sci. 2*, 1844−1852.

Rychlik, W., & Rhoads, R. (1989) *Nucleic Acids Res. 17*, 8543−8551.

Sambrook, J., Fritsch, E. F., & Maniatis, T. (1989) in *Molecular Cloning: a laboratory manual*, 2nd ed., Cold Spring Harbor Laboratory Press, Plainview, NY.

Sauer, R. T., Smith, D. L., & Johnson, A. D. (1988) *Genes Dev. 2*, 807−816.

Sharp, K. (1995) *Biopolymers 36*, 227−243.

Shortle, D., & Meeker, A. (1989) *Biochemistry 28*, 936−944.

Smith, D. L., & Johnson, A. D. (1992) *Cell 68*, 133−142.

Spolar, R. S., & Record, M. T. (1994) *Science 263*, 777−784.

Stark, M. R., & Johnson, A. D. (1994) *Nature 371*, 429−432.

Tsao, D. H. H., Gruschus, J. M., Wang, L-H., Nirenberg, M., & Ferretti, J. A. (1994) *Biochemistry 33*, 15053−15060.

Tsao, D. H. H., Gruschus, J. M., Wang, L-H., Nirenberg, M., & Ferretti, J. A. (1995) *J. Mol. Biol. 251*, 297−307.

Weiss, M. A., Ellenberger, T., Wobbe, C. R., Lee, J. P., Harrison, S. C., & Struhl, K. (1990) *Nature 347*, 575−578.

Wilson, D. S., Guenther, B., Desplan, C., & Kuriyan, J. (1995) *Cell 82*, 709−719.

Wolberger, C. (1993) *Cold Spring Harbor Symp. Quant. Biol. 58*, 159−166.

Wolberger, C. (1996) *Curr. Opin. Struct. Biol. 6*, 62−68.

Wolberger, C., Vershon, A. K., Liu, B., Johnson, A. D., & Pabo, C. O. (1991) *Cell 67*, 517−528.

BI962206B